

JOURNAL OF THE AMERICAN CHEMICAL SOCIETY

Interconversion of (*S*)-Glutamate and (2*S*,3*S*)-3-Methylaspartate: A Distinctive B₁₂-Dependent Carbon-Skeleton Rearrangement

Stacey D. Wetmore, David M. Smith, Bernard T. Golding, and Leo Radom*

Contribution from the Research School of Chemistry, Australian National University, Canberra, ACT 0200, Australia, and Department of Chemistry, University of Newcastle upon Tyne, Newcastle upon Tyne NE1 7RU, UK

Received December 12, 2000

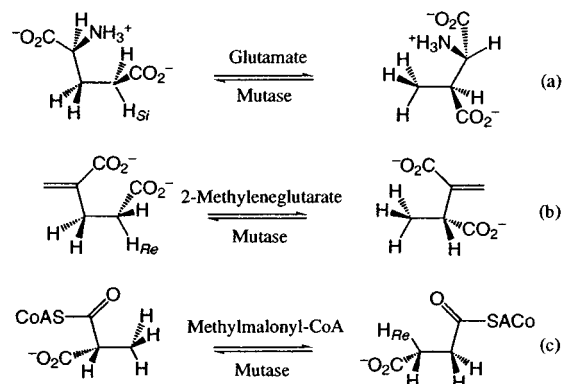
Abstract: The interconversion of (*S*)-glutamate and (2*S*,3*S*)-3-methylaspartate catalyzed by B₁₂-dependent glutamate mutase is discussed using results from high-level ab initio molecular orbital calculations. Evidence is presented regarding the possible role of coenzyme-B₁₂ in substrate activation and product formation via radical generation. Calculated electron paramagnetic resonance parameters support experimental evidence for the involvement of substrate-derived radicals and will hopefully aid the future detection of other important radical intermediates. The height of the rearrangement barrier for a fragmentation–recombination pathway, calculated with a model that includes neutral amino and carboxylic acid substituents in the migrating glyceryl group, supports recent experimental evidence for the interconversion of (*S*)-glutamate and (2*S*,3*S*)-3-methylaspartate through such a pathway. Our calculations suggest that the enzyme may facilitate the rearrangement of (*S*)-glutamate through (partial) proton-transfer processes that control the protonation state of substituents in the migrating group.

Introduction

Glutamate mutase catalyzes the conversion of (*S*)-glutamate to (2*S*,3*S*)-3-methylaspartate, a reaction which represents the first step in the fermentation of glutamate to acetate and butyrate in many clostridia.¹ Glutamate mutase, 2-methyleneglutarate mutase, and methylmalonyl-CoA mutase are the most widely studied B₁₂-dependent enzymes in a class which catalyze carbon-skeleton rearrangements (Scheme 1).^{2–4} The end result of each rearrangement is the exchange of hydrogen and a migrating group on an adjacent carbon center. The migrating groups for reactions a–c (Scheme 1) are 2-glycyl, 2-acrylate, and formyl-S-CoA, respectively.

(1) (a) Barker, H. A.; Weissbach, H.; Smyth, R. D. *Proc. Natl. Acad. Sci. U.S.A.* **1958**, *44*, 1093. (b) Barker, H. A.; Smyth, R. D.; Wilson, R. M. *Fed. Proc.* **1958**, *17*, 185. (c) Barker, H. A.; Smyth, R. D.; Wawszkiewicz, E. J.; Lee, M. N.; Wilson, R. M. *Arch. Biochem. Biophys.* **1958**, *78*, 468. (d) Barker, H. A.; Smyth, R. D.; Wawszkiewicz, E. J.; Munch-Peterson, A.; Toohey, J. I.; Ladd, J. N.; Volcani, B. E.; Wilson, R. M. *J. Biol. Chem.* **1960**, *235*, 181. (e) Buckel, W.; Barker, H. A. *J. Bacteriol.* **1974**, *117*, 1248. (f) Buckel, W. *Arch. Microbiol.* **1980**, *127*, 167.

Scheme 1. B₁₂-Dependent Carbon-Skeleton Mutases



According to the bound-free-radical hypothesis, the initial step in coenzyme B₁₂-mediated reactions is the homolytic cleavage of the cobalt–carbon bond of the enzyme, which produces the 5′-deoxyadenosyl radical and cob(II)alamin.^{2–4} The 5′-deoxy-

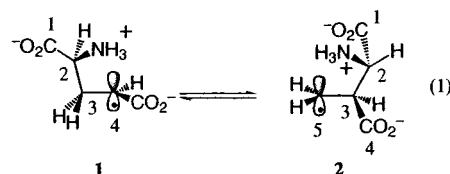
adenosyl radical abstracts 4-H_{Si} from glutamate and 4-H_{Re} from 2-methyleneglutarate and, in the reverse direction, abstracts 3-H_{Re} from succinyl-CoA.² Electron paramagnetic resonance (EPR) spectroscopy has provided an abundance of important information for developing a model for coenzyme B₁₂-mediated carbon-skeleton rearrangements² and evidence that these reactions occur through free-radical pathways.^{5,6} Subsequent to the formation of a substrate-derived radical, the migrating group moves to an adjacent carbon atom with inversion of configuration at this center for glutamate^{2,7} and 2-methyleneglutarate,² but with retention of stereochemistry for (*R*)-methylmalonyl-CoA.⁸ After the formation of the appropriate product radical, a hydrogen atom is retrieved from 5'-deoxyadenosine with the regeneration of the coenzyme.

The pathway for the radical-rearrangement step in reactions catalyzed by carbon-skeleton mutases has proved difficult to establish. One possibility is fragmentation–recombination, in which fragmentation of the substrate radical into acrylate plus a carbon-centered radical (for example, the 2-glycyl radical in the case of glutamate mutase) is followed by recombination of these species.⁶ An alternative is addition–elimination, in which intramolecular addition of the initially formed radical center to a π bond occurs with the formation of a bridged (cyclic) intermediate or transition structure.⁶ Theoretical studies on the mechanisms of action of 2-methyleneglutarate and methylmalonyl-CoA mutases indicate that the addition–elimination pathway is intrinsically more favorable in both cases and that the barrier for this pathway can be further reduced through (partial) protonation of the substrate.^{9–12} Additionally, the addition–elimination pathway for 2-methyleneglutarate mutase has been chemically modeled.¹³

The reaction catalyzed by glutamate mutase differs from those catalyzed by the other carbon-skeleton mutases because of the absence of an appropriate unsaturated linkage in the migrating group. As a consequence, the bridged structure associated with the lower energy addition–elimination pathways discovered for the other carbon-skeleton rearrangements is more difficult to conceptualize for the rearrangement of (*S*)-glutamate. In search of a “unified” low-energy mechanism, the initial generation of

an imine through reaction between the glutamate amino group and, for example, a carbonyl functionality in the protein or an additional cofactor has been postulated.^{14,15} Formation of an imine from an amino group occurs in other biological systems,¹⁶ such as the reactions catalyzed by aminomutases.¹⁷ However, there is no evidence that the appropriate groups required for such a reaction to take place are present in glutamate mutase,^{14,18,19} and the rearrangement under question has been modeled without the formation of an imine.²⁰

Despite progress in the experimental modeling of the enzymatic interconversion of glutamate and 3-methylaspartate,^{4,15,20–22} the reaction pathway is not yet definitively established. The present paper focuses on the use of high-level quantum chemical techniques to study the reaction mechanism for conversion of (*S*)-glutamate to (2*S*,3*S*)-3-methylaspartate via the related radicals (eq 1):



We would hope that comparison of the various pathways for this reaction with those previously considered for other carbon-skeleton rearrangements will yield insight into whether it is likely that all the carbon-skeleton rearrangements occur through similar pathways or whether nature has different ways to deal with these related reactions.

Computational Details

In accord with our most recent theoretical investigation of a B₁₂-mediated carbon-skeleton rearrangement,¹² all geometries were optimized at the UB3-LYP/6-31G(d,p) level. Improved reaction barriers were obtained with a method denoted G3(MP2)-RAD(p). This technique is a modification of the G3(MP2) method²³ in which a restricted-open-shell coupled-cluster calculation (URCCSD(T)/6-31G(d)) replaces the UQCISD(T)/6-31G(d) computation and the basis set extension is calculated with restricted-open-shell perturbation theory (RMP2) rather than the unrestricted formalism (UMP2). The geometries and frequencies are obtained with UB3-LYP/6-31G(d,p) rather than UHF/6-31G(d) or UMP2/6-31G(d). This procedure was chosen on the basis of the previous success of the similarly defined (G2(MP2,SVP)-RAD(p)) method^{12,24} for this type of reaction and the increased computational efficiency and accuracy of G3 relative to G2.

(14) Brecht, M.; Kellermann, J.; Plüchthun, A. *FEBS Lett.* **1993**, 319, 84.

(15) (a) Choi, S.; Dowd, P. *J. Am. Chem. Soc.* **1989**, 111, 2313. (b) Dowd, P.; Choi, S.; Duah, F.; Kaufman, C. *Tetrahedron* **1988**, 44, 2137.

(16) Metzler, D. E. *Biochemistry*; Academic Press Inc.: New York, 1977.

(17) Frey, P. A.; Reed, G. H.; Moss, M. L.; Petrovich, R. M.; Ballinger, M. D.; Lieder, K. W.; Wu, W.; Chang, C. H.; Bandarian, V.; Ruzicka, F. J.; LoBrutto, R.; Beinert, H. *Vitamin B₁₂ and B₁₂-Proteins*; Kräutler, B., Arigoni, D., Golding, B. T., Ed.; VCH, 1998; pp 435.

(18) Leutbecher, U.; Böcher, R.; Linder, D.; Buckel, W. *Eur. J. Biochem.* **1992**, 205, 759.

(19) Reitzer, R.; Gruber, K.; Jögl, G.; Wagner, U. G.; Bothe, H.; Buckel, W.; Kratky, C. *Structure* **1999**, 7, 891.

(20) Murakami, Y.; Hisaeda, Y.; Song, X.; Ohno, T. *J. Chem. Soc., Perkin. Trans. 2* **1992**, 1527.

(21) (a) Murakami, Y.; Hisaeda, Y.; Ohno, T. *Chem. Lett.* **1987**, 1357. (b) Murakami, Y.; Hisaeda, Y.; Ohno, T. *J. Chem. Soc., Chem. Commun.* **1988**, 856. (c) Murakami, Y.; Hisaeda, Y.; Ohno, T. *J. Chem. Soc., Perkin. Trans. 2* **1991**, 405.

(22) Chih, H.-W.; Marsh, E. N. G. *J. Am. Chem. Soc.* **2000**, 122, 10732.

(23) Curtiss, L. A.; Redfern, P. C.; Raghavachari, K.; Rassolov, V.; Pople, J. A. *J. Chem. Phys.* **1999**, 110, 4703.

(24) Smith, D. M.; Golding, B. T.; Radom, L. *J. Am. Chem. Soc.* **2001**, 123, 1664.

(2) (a) Buckel, W.; Golding, B. T. *Chem. Soc. Rev.* **1996**, 26, 329. (b) Buckel, W.; Bröker, G.; Bothe, H.; Pierik, A. J.; Golding, B. T. In *Chemistry & Biochemistry of B₁₂*; Banerjee, R., Ed.; Wiley-Interscience: New York, 1999; pp 757.

(3) (a) Golding, B. T.; Buckel, W. In *Comprehensive Biological Catalysis*; Sinnott, M. L., Ed.; Academic Press: London, 1997; Vol. III, pp 239. (b) Krautler, B.; Arigoni, D.; Golding, B. T. *Vitamin B₁₂ and B₁₂-Proteins*; Wiley-VCH: Weinheim, 1998.

(4) For recent reviews of the literature on glutamate mutase, see: ref 2 and Marsh, E. N. G. *Bioorg. Chem.* **2000**, 28, 176.

(5) (a) Zhao, Y.; Such, P.; Retey, J. *Angew. Chem., Int. Ed. Engl.* **1992**, 31, 215. (b) Michel, C.; Albracht, S. P. J.; Buckel, W. *Eur. J. Biochem.* **1992**, 205, 767. (c) Zelder, O.; Buckel, W. *Biol. Chem. Hoppe-Seyler* **1993**, 374, 84. (d) Zelder, O.; Beatrix, B.; Leutbecher, U.; Buckel, W. *Eur. J. Biochem.* **1994**, 226, 577. (e) Zhao, Y.; Abend, A.; Kunz, M.; Such, P.; Retey, J. *Eur. J. Biochem.* **1994**, 225, 891. (f) Padmakumar, R.; Banerjee, R. *J. Biol. Chem.* **1995**, 270, 9295.

(6) Beatrix, B.; Zelder, O.; Kröll, F. K.; Orlygsson, G.; Golding, B. T.; Buckel, W. *Angew. Chem., Int. Ed. Engl.* **1995**, 34, 2398.

(7) Munch-Peterson, A.; Barker, H. A. *J. Biol. Chem.* **1958**, 230, 649.

(8) (a) Michenfelder, M.; Hull, W. E.; Rétey, J. *Eur. J. Biochem.* **1987**, 168, 659. (b) Hull, W. E.; Michenfelder, M.; Rétey, J. *Eur. J. Biochem.* **1988**, 173, 191.

(9) Golding, B. T.; Radom, L. *J. Am. Chem. Soc.* **1976**, 98, 6331.

(10) Smith, D. M.; Golding, B. T.; Radom, L. *J. Am. Chem. Soc.* **1999**, 121, 1383.

(11) Smith, D. M.; Golding, B. T.; Radom, L. *J. Am. Chem. Soc.* **1999**, 121, 1037.

(12) Smith, D. M.; Golding, B. T.; Radom, L. *J. Am. Chem. Soc.* **1999**, 121, 9388.

(13) Ashwell, S.; Davies, A. G.; Golding, B. T.; Hay-Motherwell, R.; Mwisigye-Kibende, S. *J. Chem. Soc., Chem. Commun.* **1989**, 1483.

Useful information about radical intermediates may be obtained by comparing experimental EPR data with results obtained from quantum chemical methods. The reliable theoretical calculation of hyperfine coupling constants (HFCCs) requires an accurate description of electron correlation and a large basis set.²⁵ Among methods which account for electron correlation, density functional theory is well suited for large systems due to its reduced computational cost relative to other procedures which yield accurate couplings, such as techniques based on multireference (MRCI) or quadratic (QCI) configuration interaction.²⁵ In the present study, the HFCCs were calculated with the B3-LYP functional in conjunction with the 6-311G(2d,p) basis set, a combination which has previously been successfully employed for a variety of organic²⁶ and biologically relevant²⁷ radicals. Improvement in this basis set leads to an increased computational cost with little gain in accuracy.²⁵ This functional and basis set combination is known, in general, to slightly overestimate experimental HFCCs.^{26,28}

All calculations were performed with the GAUSSIAN 98,²⁹ MOLPRO-98,^{30a} or MOLPRO-2000^{30b} program suites. G3(MP2)-RAD(p) total energies, as well as the GAUSSIAN 98 archive entries for all optimized structures, are presented in Tables S1 and S2, respectively, of the Supporting Information.

Results and Discussion

A. Bond Dissociation Energies. Before the radical-rearrangement mechanism for (S)-glutamate is discussed, the feasibility of the radical generation step should be considered. As outlined in the Introduction, it is believed that the primary role of coenzyme B₁₂ is to generate 5'-deoxyadenosyl radicals which activate the substrate through hydrogen-atom abstraction.³¹ Additionally, the product is generated through hydrogen-atom abstraction from 5'-deoxyadenosine. We therefore begin by studying the thermodynamics of the hydrogen-transfer steps.

Information about the plausibility of the hydrogen-atom-abstraction steps in carbon-skeleton rearrangements can be

(25) (a) Eriksson, L. A. *Encyclopedia of Computational Chemistry*; Schleyer, P. v. R., Ed.; Wiley and Sons: New York, 1998. (b) Engels, B.; Eriksson, L. A.; Lunell, S. *Adv. Quant. Chem.* **1997**, *27*, 297.

(26) Eriksson, L. A. *Mol. Phys.* **1997**, *91*, 827.

(27) See for example: (a) Eriksson, L. A.; Himo, F. *Trends Phys. Chem.* **1997**, *6*, 153. (b) Wetmore, S. D.; Boyd, R. J.; Eriksson, L. A. *J. Phys. Chem. B* **1998**, *102*, 10602.

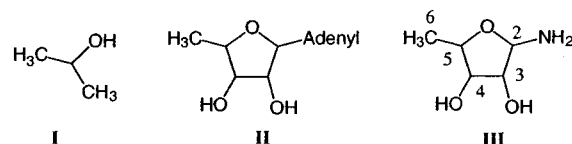
(28) We find that the HFCCs obtained at the B3-LYP/6-311G(2d,p) level are in good agreement with data obtained with the widely implemented PW-P86/6-311G(2d,p) combination. The former method slightly overestimates and the latter slightly underestimates the experimental couplings, as noted previously for a variety of organic radicals.²⁷ Due to the similarity of the results obtained with both functionals, and the widespread use of B3-LYP, only the B3-LYP results are reported in this paper.

(29) GAUSSIAN 98, Revision A.7, Frisch, M. J.; Trucks, G. W.; Schlegel, H. B.; Scuseria, G. E.; Robb, M. A.; Cheeseman, J. R.; Zakrzewski, V. G.; J. A. Montgomery, J.; Stratmann, R. E.; Burant, J. C.; Dapprich, S.; Millam, J. M.; Daniels, A. D.; Kudin, K. N.; Strain, M. C.; Farkas, O.; Tomasi, J.; Barone, V.; Cossi, M.; Cammi, R.; Mennucci, B.; Pomelli, C.; Adamo, C.; Clifford, S.; Ochterski, J.; Petersson, G. A.; Ayala, P. Y.; Cui, Q.; Morokuma, K.; Malick, D. K.; Rabuck, A. D.; Raghavachari, K.; Foresman, J. B.; Cioslowski, J.; Ortiz, J. V.; Baboul, A. G.; Stefanov, B. B.; Liu, G.; Liashenko, A.; Piskorz, P.; Komaromi, I.; Gomperts, R.; Martin, R. L.; Fox, D. J.; Keith, T.; Al-Laham, M. A.; Peng, C. Y.; Nanayakkara, A.; Gonzalez, C.; Challacombe, M.; Gill, P. M. W.; Johnson, B.; Chen, W.; Wong, M. W.; Andres, J. L.; Gonzalez, C.; Head-Gordon, M.; Replogle, E. S.; Pople, J. A.; Gaussian Inc.: Pittsburgh PA, 1998.

(30) (a) MOLPRO 98 is a package of ab initio programs written by Werner, H.-J.; Knowles, P. J. with contributions from Amos, R. D.; Berning, A.; Cooper, D. L.; Deegan, M. J. O.; Dobbyn, A. J.; Eckert, F.; Elbert, S. T.; Hampel, C.; Lindh, R.; Lloyd, A. W.; Meyer, W.; Nickless, A.; Peterson, K.; Pitzer, R.; Stone, A. J.; Taylor, P. R.; Mura, M. E.; Pulay, P.; Schütz, M.; Stoll, H.; Thorsteinsson, T. (b) MOLPRO 2000 is a package of ab initio programs written by Werner, H.-J.; Knowles, P. J. with contributions from Amos, R. D.; Bernhardsson, A.; Berning, A.; Celani, P.; Cooper, D. L.; Deegan, M. J. O.; Dobbyn, A. J.; Eckert, F.; Hampel, C.; Hetzer, G.; Korona, T.; Lindh, R.; Lloyd, A. W.; McNicholas, S. J.; Manby, F. R.; Meyer, W.; Mura, M. E.; Nicklass, A.; Palmieri, P.; Pitzer, R.; Rauhut, G.; Schütz, M.; Stoll, H.; Stone, A. J.; Tarroni, R.; Thorsteinsson, T.

(31) For criticism of this proposal, see: Dowd, P. In *Selective Hydrocarbon Activation*; Davies, J. A.; Watson, P. L.; Liebman, J. F.; Greenberg, A., Ed.; VCH: New York, 1990; p 265.

Scheme 2. The Previously Used 2-Hydroxypropane Model (**I**), 5'-Deoxyadenosine (**II**), and the Model Used In the Present Study (**III**)



obtained by considering the energy required to break the relevant C-H bonds. Despite the fact that there will be a barrier associated with hydrogen transfer between the substrate- or product-related radicals and 5'-deoxyadenosine, comparison of the BDEs that lead to the radical intermediates provides useful information regarding the thermodynamics of the hydrogen-transfer steps.

Calculations were initially performed on models of (S)-glutamate and 3-methylaspartate (equation a, Scheme 1) and the related radicals, which implement neutral carboxylic acid and NH₂ substituents to simulate the enzymatic environment.³² We have previously employed 2-hydroxypropane (**I**, Scheme 2) to model 5'-deoxyadenosine (**II**).²⁴ A more complete model, 2-amino-5-methyltetrahydrofuran-3,4-diol (**III**), which replaces the adenyl group of **II** with an amino group, is used in the present work.³³ The G3(MP2)-RAD(p) BDE for **III** is 417.7 kJ mol⁻¹, which agrees with the value previously obtained using G2(MP2,SVP)-RAD(p) for 2-hydroxypropane (**I**). This supports the appropriateness of the small model system **I**.

Comparison of the BDEs for the models of 5'-deoxyadenosine (**II**, 417.7 kJ mol⁻¹) and (S)-glutamate (382.8 kJ mol⁻¹)³² reveals that hydrogen abstraction to form the substrate-derived radical is exothermic by 34.9 kJ mol⁻¹. This supports the feasibility of hydrogen abstraction from the substrate in the overall rearrangement mechanism of (S)-glutamate.

The calculated BDE for the model for 3-methylaspartate (417.6 kJ mol⁻¹)³² indicates that hydrogen transfer from 5'-deoxyadenosine to the 3-methyleneaspartate radical is essentially a thermoneutral process. The comparable reactivity calculated for the 3-methyleneaspartate and 5'-deoxyadenosyl radicals sustains suggestions that hydrogen transfer between the product-related radical and 5'-deoxyadenosine is part of the overall rearrangement mechanism. At present, no single step in the reaction catalyzed by glutamate mutase has been identified as rate limiting.⁴ However, the formation of the substrate radical and the interconversion of substrate and product radicals have been identified as partially rate-limiting steps.^{4,34,35} Therefore, the 3-methyleneaspartate radical must acquire a hydrogen atom from 5'-deoxyadenosine relatively easily during the process of regeneration of the coenzyme, a hypothesis supported by the small calculated energy difference.

The high reactivity of the 3-methyleneaspartate radical and the significant exothermicity associated with hydrogen-atom abstraction from (S)-glutamate by the 5'-deoxyadenosyl radical both support mechanistic proposals involving hydrogen-transfer

(32) We have used neutral COOH and NH₂ substituents in our model rather than the charged COO⁻ and NH₃⁺ groups. The appropriateness of this model for the migrating group will become clear during the course of the paper. The replacement of the carboxylate attached to C4 in (S)-glutamate (eq 1) by a carboxylic acid group would also seem appropriate because of the presence of a complementary arginine at this location.¹⁹

(33) The optimized structure of our model for 5'-deoxyadenosine (**III**, Scheme 2) was obtained from a calculation starting with the appropriate configuration from the crystal structure. Since only the BDE of the exocyclic C-H bond was required in the present work, no further configurations were examined.

(34) Marsh, E. N. G. *Biochemistry* **1995**, *34*, 7542.

(35) Chih, H. W.; Marsh, E. N. G. *Biochemistry* **1999**, *38*, 13684.

steps in the conversion of (*S*)-glutamate to (2*S*,3*S*)-3-methylaspartate. The next section furnishes additional evidence that the carbon-skeleton rearrangement of (*S*)-glutamate proceeds via radical intermediates.

B. The Hyperfine Coupling Constants for the 4-Glutamyl and 3-Methyleneaspartate Radicals. A recent investigation of B₁₂-dependent glutamate mutase with a series of labeled glutamates as substrates recorded EPR signals that were determined to arise from interactions between cob(II)alamin and an organic radical approximately 6.6 ± 0.9 Å apart,³⁶ a distance in striking agreement with recent crystallographic data.¹⁹ The most abundant organic radical was concluded to be the 4-glutamyl (substrate) radical.

Because of the complexity of the EPR spectra of enzymes, the identities of the species responsible for the hyperfine structure are often not revealed directly but only through adjusting parameters (dipolar interactions, electron-electron exchange, and the Zeeman and hyperfine interactions of the radical) until the computer-simulated spectrum resembles that obtained experimentally. Additionally, in the case of the B₁₂-dependent carbon-skeleton mutases, complications arise because of potential interactions between cobalt and the organic radical. Therefore, it is useful to carry out quantum chemical calculations of the EPR parameters for the radicals potentially involved in the rearrangement mechanism for comparison with the experimental spectra. In favorable cases, this comparison could lead to the identification of the radicals that are indeed involved.³⁷

The key experimental data used to identify radicals are the hyperfine coupling constants (HFCCs) which comprise the isotropic (*A*_{iso}) and anisotropic (*T*_{xx}, *T*_{yy}, *T*_{zz}) components. The isotropic component, which yields a measure of the spin distribution at the nucleus, is difficult to calculate accurately. Theory often underestimates the experimental isotropic coupling by more than 20%. The anisotropic components, which describe the asymmetry of the spin distribution, are much easier to evaluate accurately from a computational point of view. For example, the anisotropic components of hydrogen HFCCs are often within 5–10% of the experimental values, an important result since hydrogen couplings are the data most abundant for biological systems. Only the principal HFCC tensor components for the organic radical, obtained by adding *A*_{iso} to each component of the anisotropic tensor, were reported experimentally for glutamate mutase and the uncertainty in the hyperfine couplings for isotopically labeled nuclei was estimated to be approximately 20 MHz.³⁶ Since the anisotropic components can be calculated more accurately than *A*_{iso}, we use the calculated anisotropic components of the HFCC tensor (*T*_{ii}) as our primary means of identifying radical sites.

The HFCCs calculated with B3-LYP for the 4-glutamyl, 3-methyleneaspartate, 2-glycyl, and model 5'-deoxyadenosyl radicals are presented in Table 1 (for atomic numbering, see eq 1 and Scheme 2).³² The 2-glycyl radical has been included in the present work because there is some evidence that it contributes to the EPR spectrum observed with glutamate mutase³⁶ and because of its anticipated role in the fragmentation–recombination rearrangement mechanism (see section F).²² The model for the 5'-deoxyadenosyl radical (**III**, Scheme 2) is also discussed because of its proposed role in the hydrogen-transfer steps and initiation of the radical reaction.

Table 1. Hyperfine Coupling Constants (HFCCs, B3-LYP/6-311G(2d,p), MHz) Calculated for Radicals Potentially Involved in the Rearrangement of (*S*)-Glutamate and the Experimental Couplings Extracted from Glutamate Mutase^a

radical	atom	<i>A</i> _{iso}	<i>T</i> _{xx}	<i>T</i> _{yy}	<i>T</i> _{zz}
4-glutamyl (8)	C2	52.3	-7.0	-6.5	13.5
	C3	-29.7	-2.6	0.6	2.0
	C4	59.7	-63.4	-62.7	126.1
	C5	-40.3	-5.2	0.1	5.1
	H (C4)	-51.5	-31.3	-1.9	33.2
	H (C3)	32.7	-4.3	-2.7	7.0
3-methyleneaspartate (10)	H (C3)	30.3	-4.0	-3.4	7.5
	C2	55.5	-5.0	-4.3	9.3
	C3	-35.6	-2.2	-0.3	2.6
	C4	2.1	-1.3	-0.2	1.5
	C5	76.5	-78.0	-77.4	155.4
	H (C3)	93.7	-5.1	-4.0	9.1
2-glycyl	H (C5)	-65.8	-39.3	-0.6	39.9
	H (C5)	-62.2	-39.1	-0.8	39.9
	C1	-27.2	-6.0	-2.1	8.2
	C2	29.0	-47.7	-47.1	94.7
	N	17.0	-14.2	-13.6	27.8
	H (C2)	-39.8	-24.0	-1.8	25.9
5'-deoxyadenosyl model (III)	H (N)	-3.7	-17.5	-5.4	22.9
	H (N)	-14.1	-14.2	-6.5	20.7
	C4	57.0	-7.6	-7.0	14.6
	C5	-32.3	-2.6	-0.6	3.2
	C6	76.5	-75.9	-75.3	151.2
	O	-20.7	5.1	3.7	-8.8
experiment ^b	H (C5)	31.4	-5.9	-3.8	9.7
	H (C6)	-62.1	-38.5	-0.5	39.0
	H (C6)	-61.0	-37.9	-1.1	39.0
	αH	-60.7	-30.3	-2.3	32.7
	¹³ C	86.7	-62.7	-62.7	125.3

^a For optimized structures, see Figure 4 and footnote 33. See also footnote 32. ^b Derived from the principal components of the couplings obtained from simulations of the experimental EPR spectra³⁶ using the relations $A_{ii} = A_{iso} + T_{ii}$ and $A_{iso} = 1/3\sum A_{ii}$.

The corresponding HFCCs in the 4-glutamyl (**8**) and 3-methyleneaspartate (**10**) radicals are qualitatively similar. However, there are sufficient differences in the magnitudes of the HFCCs and in the number of α- and β-hydrogens that, provided experimental resolution is adequate, the two radicals can be distinguished. For example, the carbon HFCCs for the radical centers (C4 and C5 in the 4-glutamyl and 3-methyleneaspartate radicals, respectively) differ by approximately 15–30 MHz in the isotropic and anisotropic components. This difference arises largely because of the variance in the spin density at the radical center (0.77 at C4 in **8** and 1.07 at C5 in **10**, respectively). The couplings calculated for the 2-glycyl radical fragment (**9**) and the model 5'-deoxyadenosyl radical (**III**) are also sufficiently different from those for **8** and **10** so as to allow their clear identification.

Among the radicals examined in Table 1, the agreement between the hydrogen and carbon anisotropic couplings deduced from the simulations and the results calculated with B3-LYP for the C4 hydrogen and carbon in the 4-glutamyl radical is impressive. The agreement between the isotropic components is not as good, as anticipated above, with experimental and theoretical hydrogen and carbon couplings differing by roughly 9 and 27 MHz, respectively. Our results support conclusions drawn from the isotopic-labeling studies that the 4-glutamyl radical is the primary organic radical giving rise to the experimentally observed spectra.³⁶ Additionally, we note the good agreement between the calculated β-hydrogen couplings for the substrate radical (the H(C3) couplings in **8** are approximately 30 MHz, Table 1) and those estimated in the experimental study (26 MHz).³⁸

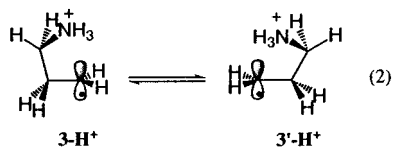
(36) Bothe, H.; Darley, D. J.; Albracht, S. P. J.; Gerfen, G. J.; Golding, B. T.; Buckel, W. *Biochemistry* **1998**, *37*, 4105.

(37) For proposals that the EPR spectra of some B₁₂-dependent enzymes arise from radicals other than substrate-related radicals, see: O'Brien, R. J.; Fox, J. A.; Kopczynski, M. G.; Babior, B. M. *J. Biol. Chem.* **1985**, *260*, 16131 and ref 5d.

The complete set of computed HFCCs for all four radicals is included in Table 1 in anticipation that the data might be used to identify other radicals involved in the rearrangement catalyzed by glutamate mutase in future EPR and related, spectroscopic studies. Comparison of the calculated couplings with those extracted using more sophisticated experimental techniques (such as electron-nuclear double resonance, ENDOR) may help to identify the additional radicals involved in the rearrangement mechanism.

The comparison of calculated and experimentally derived HFCCs, presented here for the first time, provides promising support for the formation of substrate-derived radicals in B₁₂-mediated carbon-skeleton rearrangements. On the basis of our calculations of the energy requirements for radical formation (section A) and the identity of such radicals (the present section), we can be confident that the conversion of (S)-glutamate to (2S,3S)-3-methylaspartate proceeds via free-radical intermediates. Thus, the remainder of the current work focuses on the radical-rearrangement mechanism.

C. The Rearrangement of the Aminopropyl Radical: Fragmentation–Recombination. Due to the size of the systems under investigation when carboxylate groups are present, and the extra degree of computational difficulty when dealing with flexible substituents, a smaller model system will initially be discussed. Such simplified models have been used successfully to study other carbon-skeleton rearrangements.^{11,12} Thus, the carboxylate groups in **1** and **2** are initially replaced by hydrogen atoms and the computational problem reduces to investigating the rearrangement of the protonated 3-amino-*n*-propyl radical (eq 2):



The most straightforward pathway for the conversion of (S)-glutamate to (2S,3S)-3-methylaspartate is the fragmentation–recombination pathway, which involves breaking a carbon–carbon bond to yield acrylate and a 2-glycyl radical.⁶ In the model system, the equivalent pathway results in ethylene plus the protonated aminomethyl radical (collectively referred to as **4-H⁺** in Scheme 3). Selected geometrical parameters for the species involved in the model reaction are presented in Figure 1. The G3(MP2)-RAD(p) energies are presented in Table 2.

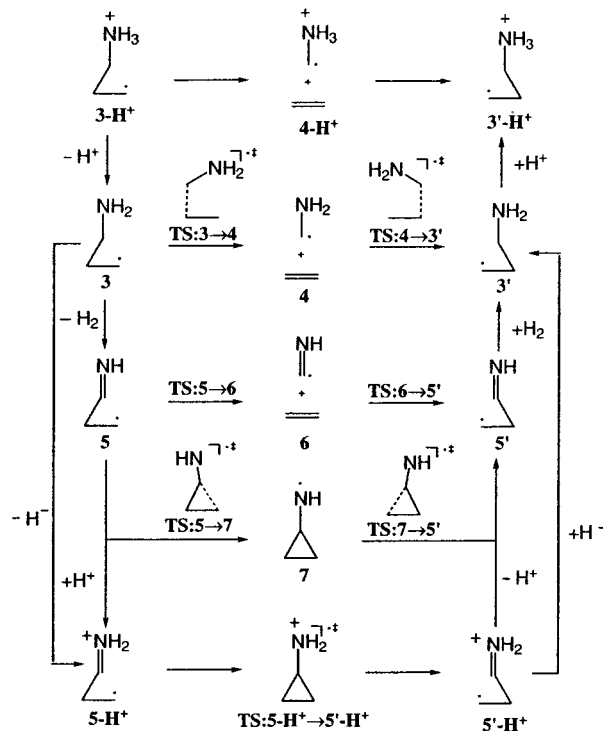
We calculate that the separated fragments **4-H⁺** are 135.5 kJ mol⁻¹ higher in energy than the protonated aminopropyl radical (**3-H⁺**). Clearly, the fragmentation–recombination barrier will be equal to or larger than this value. Because of the high energy associated with the fragments in the fragmentation–recombination pathway of **3-H⁺**, we did not feel it necessary to further characterize this surface. Qualitatively, the fragmentation–recombination pathway for **3-H⁺** is a high-energy route.

A potentially attractive possibility is that interactions between the substrate and a basic group in the enzyme may lead to (at least partial) proton transfer from the NH₃⁺ substituent (see

(38) The β -hydrogen couplings were estimated in the experimental study by varying the dihedral angles for the two hydrogen atoms adjacent to a prototypical carbon-centered radical that has an approximate spin density of 0.8 and comparing the simulated spectra incorporating these parameters with that obtained from deuterium labeling studies.

(39) Structure **3** is formally the 3-amino-*n*-propyl radical, but for reasons of simplicity, we will generally refer to it as the aminopropyl radical. Similarly, we will refer to the 3-imino-*n*-propyl radical (**5**) as the iminopropyl radical.

Scheme 3. Possible Pathways for the Degenerate Rearrangement of the Protonated Aminopropyl Radical (**3-H⁺**)³⁹



section F). Therefore, we also consider the rearrangement of the (neutral) 3-aminopropyl radical (**3**). We find that deprotonation of the migrating group in **3-H⁺** reduces the energy of the separated fragments (designated **4** in Scheme 3) by 74.4 kJ mol⁻¹ relative to the appropriate reactants. G3(MP2)-RAD(p) bond dissociation energies (BDE) for methylamine (382.0 kJ mol⁻¹) and methylammonium (445.0 kJ mol⁻¹) indicate that the calculated barrier reduction is partly due to the improved ability of NH₂ to stabilize a radical center compared with NH₃⁺ (by 63.0 kJ mol⁻¹) and partly due to the removal of unfavorable charge localization in the separated fragments **4-H⁺**. However, the barrier for fragmentation of the aminopropyl radical (**3**) is still relatively large (97.2 kJ mol⁻¹).

The high barriers associated with the fragmentation–recombination rearrangement pathways of **3-H⁺** and **3** are consistent with the high barriers calculated for the model systems used to study the rearrangement of the 2-methyleneglutarate and (R)-methylmalonyl-CoA substrate radicals.^{10,11}

D. The Rearrangement of the Iminopropyl Radical. As noted above, it has previously been proposed that interactions between a carbonyl group in the enzyme and the amino group of (S)-glutamate may lead to the formation of an imine (Schiff base) and thereby facilitate the rearrangement of the substrate by permitting the formation of a cyclic intermediate.^{14,15} This possibility, when coupled with (partial) protonation of the migrating group,^{10,11} is attractive because it would allow a mechanism analogous to that of other B₁₂-mediated carbon-skeleton mutases.

However, explicit imine formation appears unlikely since a recently reported well-resolved crystal structure shows no evidence of appropriate groups for such a process.¹⁹ The possibility that pyridoxal 5'-phosphate (a coenzyme of vitamin B₆ known to readily form imines with the amino group of amino acids) is involved in the rearrangement of (S)-glutamate has also been eliminated.⁴⁰ Indeed, it has been determined that no

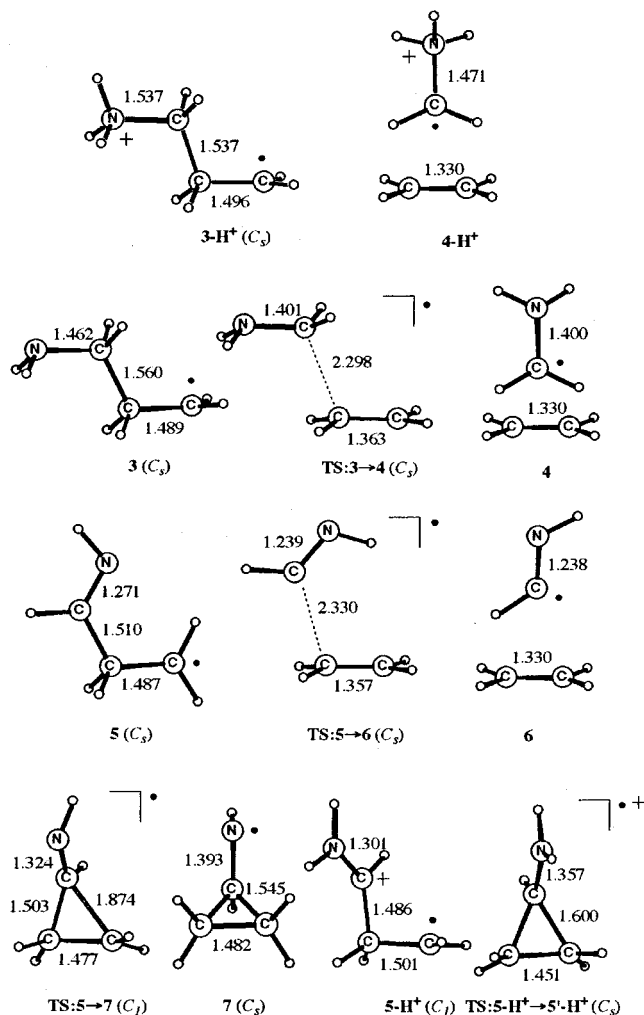


Figure 1. B3-LYP/6-31G(d,p) structures and selected bond lengths (Å) for the species involved in the degenerate rearrangement of the protonated aminopropyl radical (**3-H⁺**), aminopropyl radical (**3**), iminopropyl radical (**5**), and protonated iminopropyl radical (**5-H⁺**). See Scheme 3.

Table 2. Relative Energies (kJ mol⁻¹) for the Species Involved in the Rearrangement of the Protonated Aminopropyl Radical (**3-H⁺**, Scheme 3) and the 4-Glutamyl Radical (**8**) as Well as Related Reactions

radical	G3(MP2)-RAD(p)	radical	G3(MP2)-RAD(p)
3-H⁺	0.0	8-H⁺	0.0
4-H⁺	135.5	9-H⁺	182.5
		10-H⁺	41.7
3	0.0	8-H⁻	0.0
TS: 3→4	97.2	9-H⁻	97.7
4	61.1	10-H⁻	17.2
5	0.0	8	0.0
TS:5→6	118.0	TS: 8→9	59.9
6	90.2	9	34.7
TS:5→7	52.4	TS: 9→10	66.5
7	37.6	10	20.3
5-H⁺	0.0	11	0.0
TS: 5-H⁺→5'-H⁺	19.0	TS: 11→12	10.7
		12	10.6
		TS: 12→13	13.8
		13	2.7

cofactors other than coenzyme-B₁₂ are required by glutamate mutase.⁴¹ Additionally, attempts to trap a Schiff base by reduction with sodium borohydride have been unsuccessful.¹⁸ The inhibition of glutamate by 2-methyleneglutarate has been

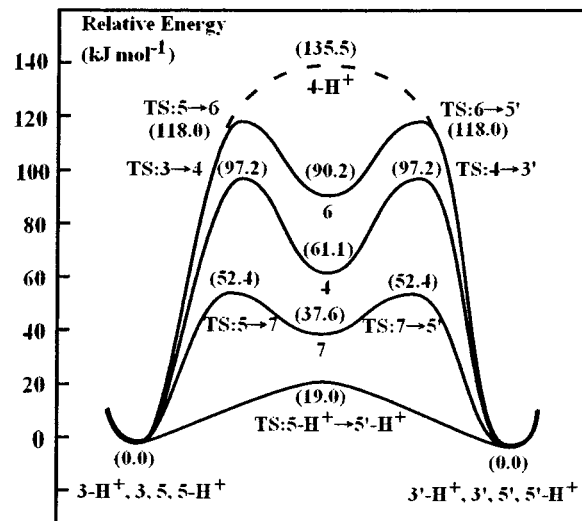


Figure 2. Schematic G3(MP2)-RAD(p) energy profile for the degenerate rearrangement of the protonated aminopropyl radical (**3-H⁺**), aminopropyl radical (**3**), iminopropyl radical (**5**), and protonated iminopropyl radical (**5-H⁺**). Relative energies (kJ mol⁻¹) in parentheses. See Scheme 3.

used as an argument for imine formation,^{14,18} but an alternative explanation has been provided to counter this proposal.² Furthermore, model studies have been carried out where migration of the 2-glycyl group was observed without the formation of an imine.²⁰

Although imine formation appears unlikely, it is still of interest to investigate the energetics of this reaction and to determine whether it provides a lower energy pathway. Three mechanistic pathways will be considered for the rearrangement of the iminopropyl radical (Scheme 3).³⁹ The relative energies for the relevant radicals are included in Table 2, and radical structures, including selected geometrical parameters, are displayed in Figure 1. The results for the iminopropyl rearrangement pathways are compared with those for the aminopropyl rearrangement in Figure 2.

(1) The Fragmentation-Recombination Pathway. One possibility for the rearrangement of iminopropyl is the fragmentation-recombination pathway, considered in the previous section for the aminopropyl radical.⁴² We find, however, that this pathway is associated with a transition structure that lies very high in energy (118.0 kJ mol⁻¹) with respect to the reactant radical (**5**). Even the separated fragments (**6**) lie 90.2 kJ mol⁻¹ above the reactant. Clearly, this pathway is even less favorable than the fragmentation-recombination of the aminopropyl radical.

(2) The Addition-Elimination Pathway. A second possible route for the rearrangement of iminopropyl involves the formation of an intermediate cyclopropylamino radical (**7**). This

(40) Suzuki, F.; Barker, H. A. *J. Biol. Chem.* **1965**, *241*, 878.

(41) Holloway, D. E.; Marsh, E. N. G. *J. Biol. Chem.* **1994**, *269*, 20425.

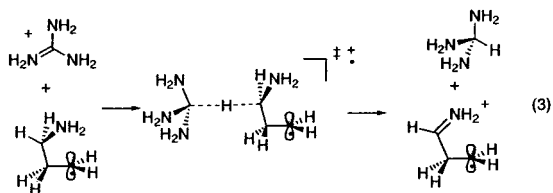
(42) The lowest energy configurations for the iminomethyl radical and the corresponding fragmentation-recombination transition structure both involve a trans orientation for the hydrogens in the imine fragment (**TS: 5→6**, Figure 1). The C_s reactant radical related to this transition structure, which involves rotation about the double bond and a 90° twist of the radical center relative to the lowest energy structure (**5**, Figure 1), lies 1.9 kJ mol⁻¹ above the lowest energy conformer at the G3(MP2)-RAD(p) level. Although there is a relatively large barrier associated with the transformation between the two C_s conformers, this barrier is less than that for fragmentation. The system will therefore have sufficient energy to overcome this rotational barrier if the transition barrier is to be crossed. Thus, the relative energies for the fragmentation-recombination pathway are reported with respect to the lowest energy C_s structure (**5**), despite the fact that rearrangement is required before the transition structure can be reached.

addition–elimination pathway involves the addition of the radical center to the imino carbon to form a cyclic intermediate (**7**) and the subsequent elimination of the imino carbon to yield the product radical (**5'**). The barrier for the addition–elimination pathway (52.4 kJ mol⁻¹) is significantly lower than the barrier for the fragmentation–recombination of the aminopropyl radical (97.2 kJ mol⁻¹). Additionally, the cyclic intermediate is only 37.6 kJ mol⁻¹ higher in energy than the reactant radical and, if formed, a small barrier (14.8 kJ mol⁻¹) leads to the product radical. Thus, an intramolecular rearrangement is clearly favored over one involving bond fragmentation for the rearrangement of the iminopropyl radical.

(3) The Protonated Pathway. A third possibility for radical rearrangement involves protonation of the reactant radical. Protonation of the migrating group has been shown to greatly facilitate concerted 1,2-shifts for related systems.^{9–12} Thus, the rearrangement of the protonated iminopropyl radical was investigated. In contrast to the addition–elimination mechanism for the neutral system, the protonated cyclic structure (**TS:5-H⁺ → 5'-H⁺**) is found to be a transition structure, rather than a reaction intermediate. However, this transition structure is calculated to lie just 19.0 kJ mol⁻¹ above the reactant radical (**5-H⁺**). Protonation of the reactant radical thus leads to a significant reduction in the barrier height (by 33.4 kJ mol⁻¹).

E. Rearrangement of the Aminopropyl Radical via Hydride Transfer. Our results above show that, in a manner similar to the rearrangement mechanisms of other carbon-skeleton rearrangements, a pathway for the rearrangement of the iminopropyl radical involving cyclization of a protonated migrating group provides a low-energy alternative to the fragmentation–recombination pathway. However, we have noted that the formation of the imine precursor in the enzyme system through reaction of the NH₂ group with some functional group within the enzyme is unlikely. In this light, it is relevant to note that the formation of a protonated imine (**5-H⁺** in the model system) can alternatively formally arise as a result of removal of a hydride ion from the parent (saturated) system (the aminopropyl radical **3** in the model system, see Scheme 3). In other words, formation of the imine **5** is not a prerequisite for formation of **5-H⁺**. The latter may be formed directly from **3**. Hydride-transfer steps have precedents in other biochemical reactions.¹⁶

The crystal structure of glutamate mutase reveals that three arginines are involved in the binding of the inhibitor.¹⁹ While one arginine has a normal type of interaction with a carboxylate group, the other two interact with the glycyl moiety in a non-standard fashion.¹⁹ A possible additional role of these arginines could be to remove the hydride ion. To examine the feasibility of the proposal of protonated imine formation through hydride ion abstraction, we modeled the removal by considering the abstraction by the guanidinium cation of a hydride ion from the neutral aminopropyl radical (eq 3):



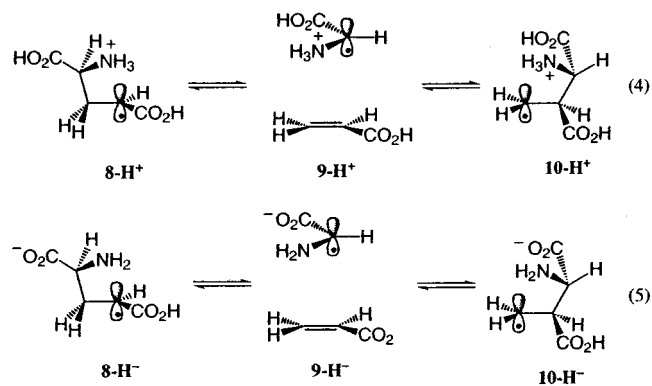
We find that the hydride-transfer reaction in eq 3 is highly endothermic (by 131.6 kJ mol⁻¹). This result implies that complete hydride transfer between the substrate and arginine is not an energetically favorable step. Thus, although the

intramolecular radical rearrangement that follows hydride removal is a lower energy pathway than fragmentation–recombination, the potentially large barrier to arrive at this rearrangement route makes this pathway less appealing. We are not aware of any experimental evidence at present for other groups within the enzyme that are better able to abstract a hydride ion.

F. The Rearrangement of the 4-Glutamyl Radical. (1) The Fragmentation–Recombination Pathway. The aminopropyl and iminopropyl model systems provide valuable mechanistic information at a low computational cost. Additionally, previous theoretical studies have shown great success using model systems.^{11,12} However, the inclusion of the carboxylate functionality in the glutamate-mutase-catalyzed reaction may lead to significant changes, partly because of its potential stabilizing effects on the separated fragments (the 2-glycyl radical and acrylic acid) generated in the fragmentation–recombination pathway and partly because the reaction is no longer thermo-neutral.

From steady-state kinetic studies on glutamate mutase, k_{cat} was determined to be 20.6 s⁻¹ at 25 °C.⁴¹ Through arguments similar to those employed previously,^{10,24,43} the barrier for the rate-limiting step in the rearrangement of (S)-glutamate is likely to lie between 60 and 75 kJ mol⁻¹. Although no single step has been identified as rate determining, the generation of the substrate radical and its conversion to the product radical are partially rate limiting.⁴ Therefore, the radical rearrangement is most probably associated with a barrier close to, or slightly smaller than, the lower bound reported above. Clearly, for the fragmentation–recombination mechanism to be plausible, the carboxylate groups must significantly reduce the rearrangement barrier relative to those calculated for the small models (**3-H⁺** and **3**).

Following our discussion for the rearrangement of the 3-aminopropyl radical, we begin by considering the effects of protonated and deprotonated substituents in the migrating group (eqs 4 and 5):



The rearrangement of **8-H⁺** (eq 4) is overall endothermic by 41.7 kJ mol⁻¹ (see Table 2 and Figure 3).⁴⁴ The energy of the separated fragments **9-H⁺** is 182.5 kJ mol⁻¹ higher than that of the reactant **8-H⁺**. Clearly, due to the high energy associated with the separated fragments, the fragmentation–recombination pathway for the rearrangement of **8-H⁺** is a high-energy route.

(43) George, P.; Glusker, J. P.; Bock, C. W. *J. Am. Chem. Soc.* **1997**, *119*, 7065.

(44) We note that the lowest energy conformations of the 4-glutamyl-related radicals (**8-H⁺**, **8-H⁻**, and **8**) and the 3-methyleneaspartate-related radicals (**10-H⁺**, **10-H⁻**, and **10**) are in accord with data from EPR studies³⁶ and with the conformation of (S,S)-tartrate observed in the crystal structure of glutamate mutase,¹⁹ respectively. See Figure 4 and Supporting Information.

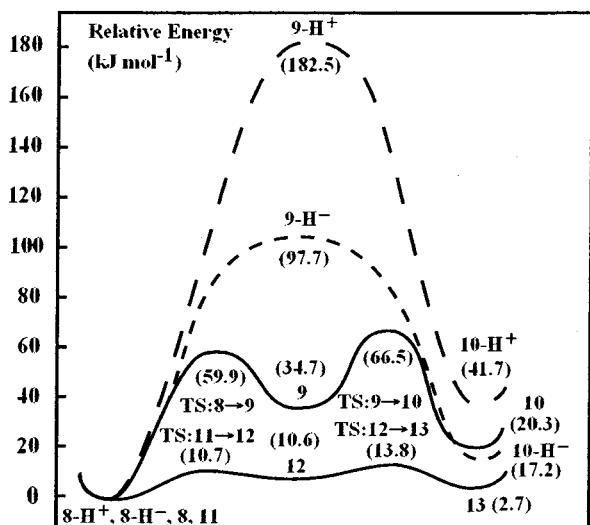
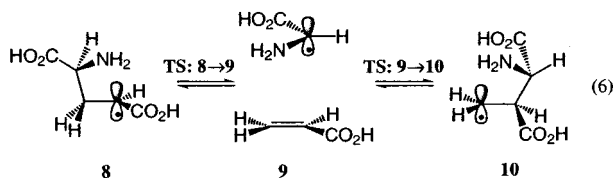


Figure 3. Schematic G3(MP2)-RAD(p) energy profile for the rearrangement of the 4-glutamyl-related radicals (8-H^+ , 8-H^- , and **8**) and the species formed by hydride ion removal (**11**). Relative energies (kJ mol^{-1}) in parentheses.

The rearrangement of 8-H^- (eq 5) is endothermic by 17.2 kJ mol^{-1} and the relative energy of the separated fragments 9-H^- is 97.7 kJ mol^{-1} (Table 2 and Figure 3).⁴⁴ Although the fragmentation–recombination barrier for 8-H^- is smaller than that for 8-H^+ , it is still significantly larger than the value estimated from the experimental results.

G3(MP2)-RAD(p) calculations show that the C–H bond dissociation energy (BDE) of neutral, protonated, and deprotonated glycine increases and therefore the stability of the related radical decreases, according to $\text{H}_2\text{NCH}_2\text{COOH}$ ($332.4 \text{ kJ mol}^{-1}$) < $\text{H}_2\text{NCH}_2\text{COO}^-$ ($363.5 \text{ kJ mol}^{-1}$) < $^+\text{H}_3\text{NCH}_2\text{COOH}$ ($420.5 \text{ kJ mol}^{-1}$). These results are in agreement with values previously reported in the literature.^{45,46} Radicals, such as the (neutral) 2-glycyl radical, that contain both a π -donor (e.g., amino) and a π -acceptor (e.g., carboxylic acid) group adjacent to the radical center are known to be synergistically stabilized,^{45–47} an effect termed captodative stabilization.⁴⁷ The synergistic stabilization is removed if the amino group of glycine is protonated, if the carboxylic acid group is deprotonated, or if both occur (as in the zwitterionic form of glycine).⁴⁵

To determine the effects of captodative stabilization on the fragmentation–recombination barrier, we consider the rearrangement of the (neutral) 4-glutamyl radical (**8**) (eq 6):



The structures and selected geometrical parameters for the radicals involved in the fragmentation–recombination pathway of **8** are presented in Figure 4.⁴⁴ The rearrangement of the 4-glutamyl radical **8** is overall endothermic by 20.3 kJ mol^{-1} (Table 2 and Figure 3).⁴⁸ Both the energy of the separated fragments (34.7 kJ mol^{-1}) and the barrier to fragmentation (59.9

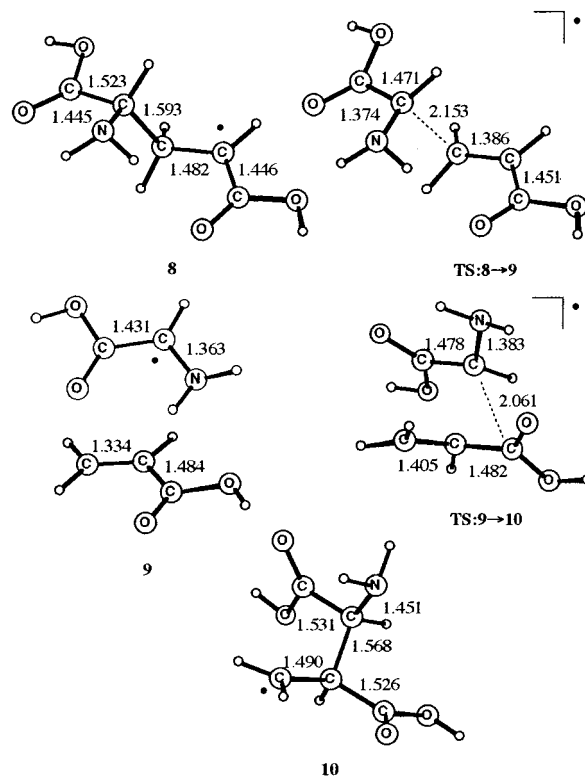


Figure 4. B3-LYP/6-31G(d,p) structures and selected bond lengths (\AA) for the species involved in the fragmentation–recombination pathway for the rearrangement of the 4-glutamyl radical (**8**). All species have C_1 symmetry.

kJ mol^{-1}) for the system with neutral carboxylic acid and amino groups are significantly smaller than those obtained for our models with a protonated or deprotonated migrating group (8-H^+ and 8-H^-), as well as our model that neglects the carboxylate functionality (**3**).

Our results indicate that the fragmentation–recombination barrier for the neutral 4-glutamyl radical is significantly less than those for the protonated and deprotonated forms. This may be attributed to the greatly increased stability of the fragment glycyl radical, as well as the removal of the unfavorable localization of charge that is present in the separated fragments related to the corresponding protonated and deprotonated substrates. The latter effect is likely to be less important in the enzymatic environment than in our gas-phase calculations. However, the increase in the radical stability that occurs upon deprotonation of the NH_3^+ group (88.1 kJ mol^{-1}) and protonation of the COO^- substituent (31.1 kJ mol^{-1}) is sufficiently large that a reduction in the fragmentation–recombination barrier should accompany these modifications to the migrating group within the enzyme, even if electrostatic effects are insignificant. The significant captodative stabilization provided by the neutral amino and carboxylic acid substituents in the glycyl fragment leads to a rearrangement barrier that lies within the range estimated for the B_{12} -catalyzed rearrangement of (*S*)-glutamate. We also note that previous calculations for a related carbon-skeleton rearrangement (modeling the methylmalonyl-CoA mutase reaction) have shown that a continuum exists between the unassisted (in this case, addition–elimination) pathway and the fully protonated pathway.^{10,12} Therefore, we suggest that partial-proton-transfer processes involving appropri-

(45) Yu, D.; Rauk, A.; Armstrong, D. A. *J. Am. Chem. Soc.* **1995**, *117*, 1789.

(46) Leroy, G.; Sana, M.; Wilante, C. *J. Mol. Struct.* **1991**, *228*, 37.

(47) (a) Viehe, H.-G.; Janousek, Z.; Merényi, R.; Stella, L. *Acc. Chem. Res.* **1985**, *18*, 148. (b) Sustmann, R.; Korth, H. G. *Adv. Phys. Org. Chem.* **1990**, *26*, 131.

(48) This is consistent with the stabilizing effect of a carboxylic acid substituent adjacent to a radical center, as found also in the related rearrangement of the (*R*)-methylmalonyl-CoA-derived radical.¹²

ate hydrogen bonds to the migrating group may also lead to a barrier reduction for the rearrangement of the 4-glutamyl radical.

The most well-defined crystal structure of glutamate mutase indicates that the inhibitor is tightly bound at the active site through a series of hydrogen bonds with more than 14 amino acid residues.¹⁹ It has been suggested that these hydrogen bonds may yield a favorable environment for a fragmentation–recombination pathway by preventing total separation of the two fragments,¹⁹ thus catalyzing the reaction on an entropic basis. This tight arrangement could also serve to prevent side reactions of the highly reactive intermediates with, for example, surrounding amino acids. This role of the enzyme has been termed “negative catalysis”.⁴⁹

Although prevention of complete separation of the fragmentation products and hindrance of side reactions are important roles for the enzyme, we propose that the enzyme plays an additional role by stabilizing the fragments in the fragmentation–recombination pathway. Our calculations suggest that this may be accomplished through (partial) proton-transfer processes that control the protonation state of the migrating glyceryl group, i.e., (partial) deprotonation of the NH_3^+ group and (partial) protonation of the COO^- substituent. It is important to note that at neutral pH glutamate is likely to be present in its zwitterionic form, and therefore this is also likely to be the best initial representation of the glyceryl substituent.

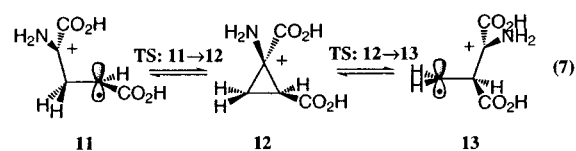
Typically, one arginine group within the enzyme interacts with one carboxylate group in the substrate. This has been previously noted for the substrates of 2-methyleneglutarate and methylmalonyl-CoA mutases and is the situation for the carboxylate group at C4 in (S)-glutamate (eq 1). However, the crystal structure of glutamate mutase reveals that there are two arginine residues interacting with the carboxylate substituent in the migrating group of the substrate in a nonstandard fashion.¹⁹ It is possible that the role of these arginines (the “arginine claw”) is to protonate (at least partially) this carboxylate group. Furthermore, although the NH_3^+ group in (S)-glutamate has been replaced by a hydroxyl group in the inhibitor,¹⁹ the crystal structure does reveal a number of amino acid residues capable of acting as proton acceptors from the NH_3^+ group of the substrate. In particular, Gly1171 is in an ideal position to accept a hydrogen bond and thus to deprotonate (at least partially) the NH_3^+ substituent. The phenol oxygens of Tyr1177 and Tyr1181, as well as the backbone oxygen of His1150, are also in a position to accept hydrogen bonds from the NH_3^+ substituent. It is important to keep in mind that the glyceryl radical is likely to have quite different pK_a values from glycine itself. Specifically, the amino group is less likely to be protonated and the carboxylic acid group is less likely to be deprotonated in the glyceryl radical than in glycine because of the captodative stabilization in the neutral radical noted above.⁵⁰ Thus, the proposed (partial) proton transfers are more likely to occur after the homolytic cleavage of the C–C bond of the substrate.

In summary, our results support recent experimental evidence^{4,22} for the interconversion of (S)-glutamate and (2S,3S)-3-methylaspartate in the presence of glutamate mutase through a fragmentation–recombination pathway. Compared with the fragmentation–recombination pathways for the rearrangement

of 2-methyleneglutarate and (R)-methylmalonyl-CoA radicals where the calculated barrier heights are significantly larger, such a mechanism is much more plausible for the rearrangement of (S)-glutamate. Our calculations indicate that the enzyme may make this otherwise high-energy pathway favorable in the case of (S)-glutamate by (partially) deprotonating the NH_3^+ group and (partially) protonating the COO^- substituent in the migrating glyceryl moiety. In a similar fashion to our proposal that methylmalonyl-CoA mutase catalyzes the rearrangement of (R)-methylmalonyl-CoA by partial-proton-transfer,^{12,51} we propose here that glutamate mutase also uses (partial) proton-transfer processes to catalyze the interconversion of (S)-glutamate and (2S,3S)-3-methylaspartate.

(2) Removal of a Hydride Ion. Despite the fact that the (S)-glutamate fragmentation barrier height is within the range expected for B_{12} -assisted rearrangements, it is interesting to explore whether the reaction barrier may be further reduced. The direct migration of the glyceryl residue through a bridged species is not expected due to the anticipated high energy associated with this type of transition structure. Indeed, our attempts to locate a bridged transition structure in the present work were unsuccessful.

Our studies of the small model system (**5-H⁺**) described above show that the rearrangement of a protonated imine through a cyclic structure corresponds to a low-energy rearrangement pathway. More specifically, the barrier for the rearrangement of the protonated iminopropyl radical (**5-H⁺**) is smaller than the barrier calculated for the fragmentation–recombination pathway of the aminopropyl radical (**3**). In the larger model system, we have located minimum energy structures for the 4-glutamyl (**8**) and 3-methyleneaspartate (**10**) radicals in which the relevant carbon–hydrogen bond is significantly lengthened.⁵² These alternative structures of the parent radicals could aid the formation of the related protonated imines through reduction of the barrier for hydride ion removal. Thus, although hydride transfer can be associated with a large barrier (section E), it is still of interest to investigate the effects of the carboxylic acid groups on the resulting intramolecular rearrangement barrier (eq 7).



The reaction depicted in eq 7 is calculated to be slightly endothermic (by 2.7 kJ mol^{-1} , Table 2).⁵³ The skeletal structures of **TS:5-H⁺** \rightarrow **5'-H⁺** (Scheme 3) and **12** (reaction 7) are quite similar, but the former is a transition structure while the latter is an intermediate, which lies in an extremely shallow energy well. In a manner similar to that found for the small model system, the barrier in reaction 7 (13.8 kJ mol^{-1}) is much smaller than that calculated for the fragmentation–recombination pathway (65.5 kJ mol^{-1} for reaction 6). The schematic energy profile for this reaction pathway is compared with that for the fragmentation–recombination alternative in Figure 3.

(51) Experimental support for the importance of partial-proton-transfer has recently been reported: (a) Maiti, N.; Widjaja, L.; Banerjee, R. *J. Biol. Chem.* **1999**, *274*, 32733. (b) Thomä, N.; Evans, P. R.; Leadlay, P. F. *Biochemistry* **2000**, *39*, 9213.

(52) At the B3-LYP/6-31G(d,p) level, the conformers with C–H bonds lengthened to approximately 1.105 Å are only 3.3 and 0.1 kJ mol^{-1} , respectively, higher in energy than the lowest energy conformers of the 4-glutamyl (**8**) and 3-methyleneaspartate (**10**) radicals, which both have C–H bond lengths of 1.096 Å. Both conformers involve a staggered arrangement of the amino hydrogens about the C–H bond of interest.

(49) Rétey, J. *Angew. Chem., Int. Ed. Engl.* **1990**, *29*, 355.

(50) One possible quantitative measure of this effect comes from the differences in the calculated BDEs of neutral, protonated, and deprotonated glycine. The BDEs reveal that proton transfer from the protonated glyceryl radical to neutral glycine is exothermic by 88.1 kJ mol^{-1} , while proton transfer from neutral glycine to the deprotonated glyceryl radical is exothermic by 31.1 kJ mol^{-1} .

The low calculated barrier for reaction 7 indicates that, for the gas-phase reaction, the rearrangement of the (*S*)-glutamate radical via a cyclic intermediate following removal of a hydride ion is a considerably lower energy process than rearrangement via a fragmentation–recombination pathway. It is interesting that the end result of such a hydride transfer in the glutamate-mutase-catalyzed reaction would be a mode of rearrangement similar to that resulting from protonation of the substrate in the reactions catalyzed by 2-methyleneglutarate mutase and methylmalonyl-CoA mutase. However, as we have previously noted, the barrier for the initial hydride transfer is likely to significantly exceed that of fragmentation–recombination, and there is no direct experimental evidence in support of such a mechanism at the present time.

Conclusions

Comparison of bond dissociation energies of models for (*S*)-glutamate, (2*S*,3*S*)-3-methylaspartate, and 5'-deoxyadenosine obtained from high-level *ab initio* calculations provides support for substrate activation and product formation through hydrogen-atom transfer to or from coenzyme-B₁₂. Furthermore, the hyperfine coupling constants calculated for the substrate (4-glutamyl) radical are in good agreement with experimental data obtained from the EPR spectrum of glutamate mutase. These data not only help substantiate that the interconversion of (*S*)-glutamate and (2*S*,3*S*)-3-methylaspartate occurs through a pathway involving free radicals but they may also aid the future identification of the additional radicals involved.

We find that the fragmentation–recombination barrier for the rearrangement of (*S*)-glutamate is highly dependent on the stability of the fragment radical. Our calculations show that the reaction benefits from a synergistic effect on the stability of the migrating glycylyl group of the substrate of deprotonation of the NH₃⁺ group and protonation of the COO[−] substituent. These

(53) The relative energies for the species in eq 7 are reported with respect to a C₁ conformer for the reactant radical (**11**). A lower energy C_s conformer was also found in the present work, in which there is hydrogen bonding between the amino group and the carbonyl oxygen of the carboxylic acid group at the radical center (i.e., achieved by rotation at both the cationic and radical centers in **11** by approximately 90°). This conformer is 36.9 kJ mol^{−1} lower in energy at the G3(MP2)-RAD(p) level than **11** (44.1 kJ mol^{−1} at the B3-LYP/6-31G(d,p) level). However, since carboxylate groups are known to be involved in hydrogen bonding with arginine residues in the protein, the significant distortions required for the formation of this C_s radical from the parent system are questionable. Additionally, it may be difficult for such a twisted conformer to fit into the active site of the enzyme. Thus, we report relative energies in terms of the more relevant, but higher energy, structure (**11**) that does not involve intramolecular hydrogen-bonding interactions.

results suggest that the enzyme may catalyze the rearrangement of (*S*)-glutamate by controlling the protonation state of the migrating group through appropriate (partial) proton-transfer processes, i.e., by (partially) deprotonating the NH₃⁺ group and (partially) protonating the COO[−] substituent. The intricate hydrogen-bonding network that encompasses the substrate within the active site provides a suitable environment to fulfill this requirement, and groups capable of these actions have been proposed. Our results support recent experimental evidence for the interconversion of (*S*)-glutamate and (2*S*,3*S*)-3-methylaspartate assisted by glutamate mutase through a fragmentation–recombination pathway.

The glutamate mutase carbon-skeleton rearrangement differs from those catalyzed by other carbon-skeleton mutases through the absence of an unsaturated linkage in the migrating group and the potential for greater relative stability of the separated fragments in the fragmentation–recombination pathway. Because of these differences, it would seem that different pathways are exploited for the different B₁₂-catalyzed carbon-skeleton rearrangements.

There is nevertheless an intriguing link between our proposed mechanism for glutamate mutase and that for other B₁₂-mediated carbon-skeleton rearrangements, such as methylmalonyl-CoA mutase. In the latter case, protonation of the migrating group facilitates the rearrangement, and the enzyme serves to *enhance* the extent of protonation by partial-proton-transfer. On the other hand, in the glutamate mutase situation, protonation of the amino group of the glycylyl fragment is unfavorable, and the enzyme serves to *reduce* this by partial-proton-transfer. Thus, a potential common role for carbon-skeleton-mutases is mediation of otherwise difficult radical rearrangements through (partial) proton-transfer processes.

Acknowledgment. We gratefully acknowledge generous grants of computer time on the Fujitsu VPP300 and the SGI Power Challenge of the ANU Supercomputing Facility. S.D.W. wishes to thank the Natural Sciences and Engineering Research Council of Canada (NSERC) for financial support and the ANU for a Visiting Fellowship. We thank Dr. Michael Collins for extensive helpful discussions and an anonymous referee for insightful comments.

Supporting Information Available: G3(MP2)-RAD(p) total energies (Table S1) and GAUSSIAN 98 archive entries for the RMP2/6-31G(d)//B3-LYP/6-31G(d,p) calculations for all relevant structures (Table S2). This information is available free of charge via the Internet at <http://pubs.acs.org>.

JA004246F